JOC The Journal of Organic Chemistry

Article

pubs.acs.org/joc

Accelerated Submonomer Solid-Phase Synthesis of Peptoids Incorporating Multiple Substituted *N*-Aryl Glycine Monomers

Caroline Proulx, Stan Yoo, Michael D. Connolly, and Ronald N. Zuckermann*

The Molecular Foundry, Lawrence Berkeley National Laboratory, 1 Cyclotron Road, Berkeley, California 94720, United States

Supporting Information

ABSTRACT: *N*-Aryl glycines are a chemically diverse class of peptoid monomers that have strong structure-inducing propensities. Yet their use has been limited due to the sluggish reactivity of the weakly nucleophilic aniline submonomers. Here, we report up to a 76-fold rate acceleration of the displacement reaction using aniline submonomers in solid-phase peptoid synthesis. This is achieved by adding halophilic silver salts to the displacement reaction, facilitating bromide abstraction and AgBr precipitation. Mechanistic insight derived from analysis of a series of 15 substituted anilines reveals that the silver-mediated reaction proceeds through a transition state that has considerably less positive charge buildup on the incoming nucleophile and an enhanced leaving group. This straightforward enhancement to the submonomer method enables the rapid room temperature synthesis of a wide variety of *N*-aryl glycine-rich peptoid oligomers, possessing both electron-withdrawing and -donating substituents, in good yields.

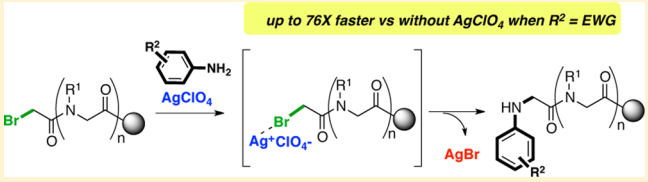

INTRODUCTION

Peptoids are biomimetic polymers composed of *N*-substituted glycine repeating units.[1] Structurally, peptoid monomers differ from naturally occurring amino acids by the point of attachment of the side chains, located at the nitrogen atom instead of the α-carbon (Figure 1a). This causes simultaneous loss of the chiral center and the backbone hydrogen-bond donor (*N*H). This results in (a) an increased stability to proteases;[2] (b) enhanced chemical diversity, owing to an efficient two-step automated submonomer synthesis cycle combining readily available primary amines and bromoacetic acid (Figure 1b);[3] and (c) fundamental differences in the rules that govern their conformation, folding, and self-assembly.[4] These structural differences result in a unique system, where local conformational order and self-assembly properties are primarily dictated by side-chain functionality and sequence patterning. To expand and modulate existing secondary structures accessible to peptoid oligomers while retaining chemical diversity, strategies are required to improve backbone conformational control and strengthen noncovalent side chain−side chain interactions. Aromatic interactions have played a central role in enforcing a wide variety of peptoid structures, including ribbons,[5] threaded loops,[6] helices,[7] superhelices,[8] and two-dimensional peptoid nanosheets.[9] In all of these examples, the composition of the peptoid sequences contained ≥50% aromatic monomers. Furthermore, *N*-aryl glycines, where the phenyl ring is directly attached to the peptoid backbone nitrogen, have been shown to strongly induce a *trans* backbone amide bond geometry.[5,10] More generally, aromatic interactions are well-known to play powerful roles in molecular recognition events[11] and in driving supramolecular assembly,[12] placing importance on their incorporation into peptoids in high yields.

The design of sophisticated peptoid secondary structures requires precise control of backbone and side-chain dihedral angle geometries. In that respect, both steric and electronic effects have played pivotal roles in reducing tertiary amide isomerization (ω) and restricting the rotation of the backbone Φ and ψ dihedral angles in *N*-substituted glycines (Figure 1c). For example, bulky, chiral aromatic side chains [e.g., (*S*)-*N*-(1-phenylethyl)glycine (*N*spe),[7a] (*S*)-*N*-1-(1-naphthylethyl)-glycine (*N*s1npe),[5,7b,10a] and *N*-(*t*-butyl)glycine (*Nt*Bu)][13] residues have been shown to favor the less sterically encumbered *cis* amide bond geometry ($\omega \approx 0°$), while *N*-(aryl)glycines,[5,10] *N*-(alkoxy)glycine,[14] *N*-(hydroxyl)glycine,[15] and *N*-(acylhydrazide)glycine[16] monomers enforce the *trans* amide bond configuration ($\omega \approx 180°$).

Precise patterning of these structure-inducing residues in peptoid sequences has resulted in stabilization of secondary structures. More specifically, *N*spe and *N*s1npe-containing oligomers have been shown to induce polyproline type I (PPI)-like helices and threaded loops secondary structures.[6,7] In these systems, ring substitution with electron-deficient groups (e.g., pentafluoro and nitro) has been extensively studied, revealing important effects on secondary structure and noncovalent n→π^*_{Ar} interactions in model systems.[17] Moreover, alternating *N*-aryl/*N*s1npe sequences have provided peptoid ribbon structures,[5,10a] and the strategic incorporation of hydrogen bond donors/acceptors in *N*-aryl side chains has given access to turn-like secondary structures.[10c] In addition to rotational restrictions in the backbone dihedral angles, the χ^1 side-chain dihedral angle in *N*-aryl glycines is restricted to $\chi^1 \approx 90°$, as observed in X-ray crystal structures and predicted by molecular

Received: June 25, 2015
Published: August 17, 2015

DOI: 10.1021/acs.joc.5b01449
J. Org. Chem. 2015, 80, 10490−10497

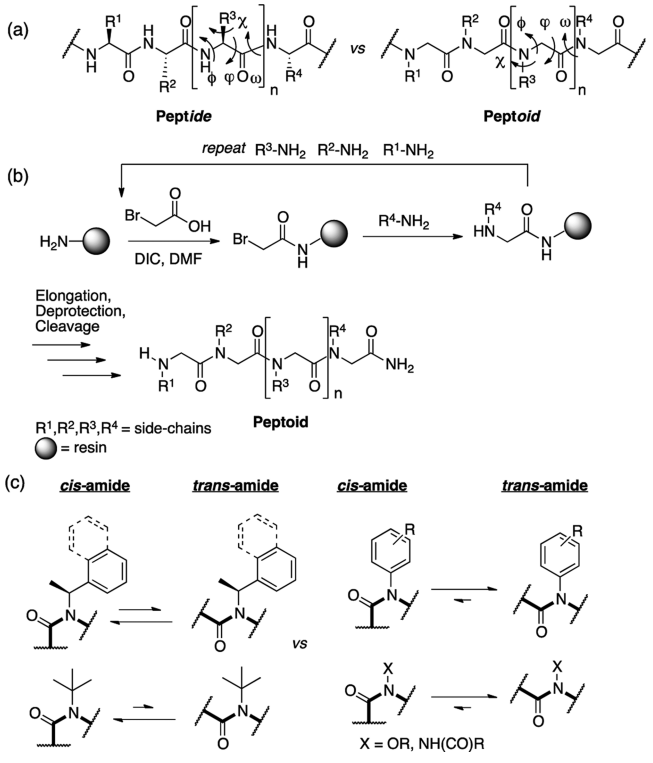

Figure 1. (a) Peptide vs peptoid structure. (b) Solid-phase submonomer peptoid synthesis method. (c) Strategies to restrict amide bond rotation in peptoids by incorporating α-chiral aromatic and *tert*-butyl side chains (left) and aryl, hydroxyl, and hydrazide side chains (right), to favor *cis* and *trans* backbone amide configurations, respectively.

modeling.[10b] Incorporation of bulky *ortho*-substituents in *N*-aryl glycine monomers has yielded atropisomers that can be separated using chiral HPLC.[10a,d]

Despite the critical ability of *N*-aryl glycine residues to induce local structure in peptoids, their incorporation has been plagued by low yields, due to the low nucleophilicity of anilines during the displacement step of submonomer peptoid synthesis. This issue has led to the use of prolonged (~16 h) displacement times,[18] microwave irradiation,[10c] or solution-phase synthesis methods,[5] which has limited their use, especially in longer oligomers. Furthermore, incorporation of electron-deficient anilines, which would allow strengthening of $\pi-\pi$ side-chain interactions in peptoids with *trans*-amide configurations, has not been attempted beyond incorporation of a single *N*-(4-fluorophenyl)glycine[5] or *N*-(4-hydroxy-3-nitrophenyl)glycine monomer[10b] in an alternating *N*-aryl glycine/*N*s1npe hexapeptoid or *N*-aryl tripeptoid, respectively. Computational studies of model *N*-methylacetanilides with electron-withdrawing groups revealed a maintained preference for the *trans* amide bond configuration.[10b]

Faced with the ever-present challenge of incorporating weak nucleophiles into peptoids using the submonomer method, we aimed to develop a general approach to accelerate this reaction. Toward that end, we focused on ways to facilitate the abstraction of the halide during the displacement step. Here, we report that the addition of silver salts during the displacement step enhances reaction rates by up to 76-fold with a series of aniline submonomers bearing both electron-rich and electron-poor substituents. We further report the efficient synthesis of amphiphilic peptoids up to 12 residues in length, possessing up to six *N*-aryl glycine monomers.

RESULTS AND DISCUSSION

Reaction Optimization and Scope. The halophilicity of silver salts has been used previously to promote a variety of reactions through irreversible abstraction of halides from halogen−carbon bonds to form insoluble precipitates (AgX).[19] For example, nucleophilic substitution reactions involving alkyl halides,[20] cross-coupling reactions via halide abstraction from a metal catalyst,[21] and rearrangements[22] have all been promoted by addition of silver salts. For example, the solvolysis of ethyl bromide showed >5000-fold rate enhancement when assisted by silver salts.[23] However, surprisingly little is known about the impact of silver salts on displacement reactions with α-haloacetamides, in analogy to the submonomer peptoid synthesis displacement reaction. In the closest reported example, the rate of solvolysis of phenacyl bromide in aqueous ethanol in the presence of $AgClO_4$ was enhanced by >500-fold as compared to the reaction without silver.[23]

Inspired by these results, we investigated the impact of silver perchlorate on the displacement of resin-bound bromoacetylated peptoids with aniline submonomers. Model bromoacetylated tetrapeptoid **2** was synthesized and treated on resin with 4-(CF_3)aniline as a representative electron-poor aniline in the presence of 3 equiv of $AgClO_4$ in different solvents (Table 1).

Table 1. Optimization of the Displacement Reaction Using 4-(Trifluoromethyl)aniline

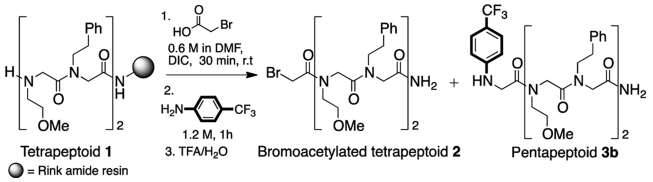

entry	solvent	$AgClO_4$ (no. of equiv)[a]	conversion to **3b** after 1 h (%)[b]
1	DMF	n/a	17
2	DMF	3.0	42
3	NMP	n/a	16
4	NMP	3.0	32
5	MeCN	n/a	25
6	MeCN	3.0	25
7	THF	n/a	17
8	THF	3.0	97
9	THF	1.0	70

[a]Based on resin loading. [b]Conversions = [(area of **3**)/(area of **2** + **3**)] × 100, where the areas are obtained from peaks on analytical HPLC traces with the absorbance at 214 nm.

To favor a presumed S_N2-type displacement mechanism, polar aprotic solvents were screened, such as *N*,*N*′-dimethylformamide (DMF), *N*-methyl-2-pyrrolidone (NMP), acetonitrile (MeCN), and tetrahydrofuran (THF). Using THF, completion of the reaction was observed after 1 h as detected by HPLC (Figure 2a). The slower reactivity of silver-assisted displacement reactions in NMP, DMF, and MeCN may be due in part to solvent complexation with silver perchlorate, as well as poor resin swelling in the case of acetonitrile.[24] Performing the same reaction in NMP or THF without addition of $AgClO_4$ provided only 15% and 17% conversion to the desired product, respectively (Figure 2b).

DOI: 10.1021/acs.joc.5b01449
J. Org. Chem. 2015, 80, 10490−10497

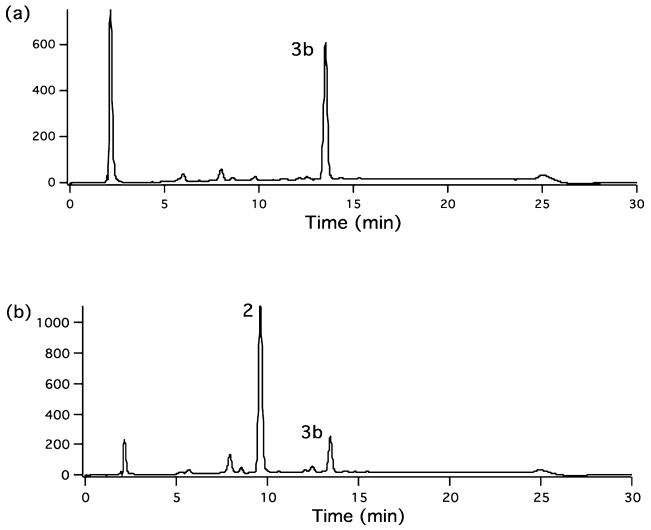

Figure 2. Representative analytical HPLC traces after 1 h displacement of compound **2** with (a) 1.2 M 4-(CF_3)aniline in THF with 3 equiv of $AgClO_4$ and (b) 1.2 M 4-(CF_3)aniline in THF, followed by cleavage from the resin.

With these optimized conditions in hand, we next screened a series of 3- and 4-substituted anilines possessing both electron-donating groups (EDG) and electron-withdrawing groups (EWG) (Table 2). Specifically, resin-bound bromoacetylated tetrapeptoid **2** was treated with a 1.2 M solution of aniline in THF and 3 equiv of $AgClO_4$ for 1 h (**3a**–**g**) and compared with resin that was treated with a standard 1.2 M solution of aniline in NMP. Most electron-poor anilines afforded the desired *N*-aryl glycine-terminated peptoid in >95% conversions after 1 h in the presence of silver perchlorate. For example, reaction with 4-aminobenzophenone was complete in 1 h in the presence of $AgClO_4$ in THF, whereas only 10% conversion to the desired product was detected using standard conditions (see Table 2, **3d**). This enables a dramatic reduction in displacement times with electron-poor aniline nucleophiles. Of note, visible formation of an AgBr precipitate was observed during the course of the reaction. However, the precipitate was solubilized in the subsequent acylation reaction (0.6 M bromoacetic acid and DIC) in the monomer addition cycle, such that its formation did not impede solid-phase synthesis of longer peptoid oligomers (see SI).[25]

Table 2. Comparative Conversions of Bromoacetylated Tetrapeptoid 2 to the Desired *N*-Aryl Glycine-Containing Pentapeptoid with and without Addition of $AgClO_4$ for Substituted Anilines with $\sigma \geq 0$

	aniline	σ	% conversion[a] to **3** with silver	% conversion to **3** without silver
3a	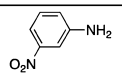	0.710	97.1 ± 0.90[b]	22.7 ± 4.4[b]
3b	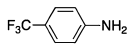	0.540	95.6 ± 2.2[b]	16.8 ± 1.7[b]
3c	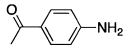	0.502	97.9 ± 0.32[b]	11.7 ± 1.3[b]
3d	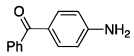	0.430	95.2 ± 3.8[b]	10.2 ± 0.38[b]
3e	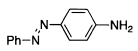	0.390	87.5 ± 0.95[b]	18.2 ± 1.4[b]
3f	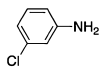	0.373	97.6 ± 0.19[b]	59.1 ± 0.27[b]
3g	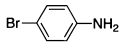	0.232	96.8 ± 0.06[b]	71.9 ± 3.9[b]
3h	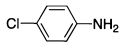	0.227	97.7 ± 0.77[c]	40.4 ± 4.1[c]
3i	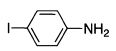	0.180	93.0 ± 1.0[c]	30.8 ± 0.76[c]
3j	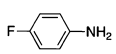	0.062	98.2 ± 1.0[c]	75.2 ± 2.2[c]
3k	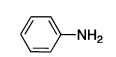	0	97.2 ± 0.04[c]	66.9 ± 0.67[c]

[a]Conversions = [(area of **3**)/(area of **2** + **3**)] × 100, where the areas are obtained from peaks on analytical HPLC traces with absorbance at 214 nm. [b]Reaction was stopped after 60 min. [c]Reaction was stopped after 15 min.

Synthesis of Glyoxyl-Terminated Peptoids. Displacement reactions using anilines with moderately electron-withdrawing substituents (Hammett constant $0 \leq \sigma \leq 0.227$, Table 2, **3h**–**3k**) were complete in only 15 min with addition of $AgClO_4$. However, upon prolonged treatment with $AgClO_4$ (1–2 h), these substrates underwent a silver-promoted oxidation of the *N*-terminal *N*-aryl glycine residue. Imine hydrolysis during cleavage of the peptoid from the resin then afforded a glyoxyl-terminated peptoid and tetrapeptoid decomposition product exclusively, as detected by LCMS (see Supporting Information (SI)). The structure of the α-oxo aldehyde functional group was further confirmed by synthesizing tetrapeptoid **4**, containing an *N*-terminal *N*-(2-aminoethyl)-glycine. After addition and silver-catalyzed oxidation of an *N*-(4-methoxyphenyl)glycine residue to give **5**, this substrate underwent an intramolecular cyclization reaction to afford heterocycle-terminated peptoid **7** (Scheme 1).

Scheme 1. Silver-Promoted Oxidation of *N*-(4-Methoxyphenyl)glycine-Terminated Peptoid 4, Followed by Intramolecular Cyclization To Give 7

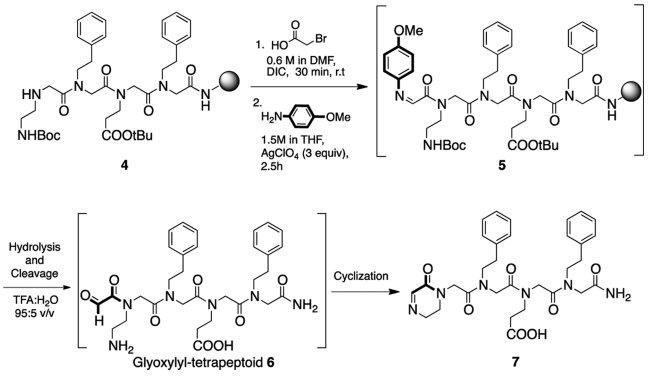

With aniline substrates containing electron-donating substituents, addition of silver salt was deemed unnecessary, as complete conversion to the desired product was observed by HPLC after a 10–15 min reaction time using 1.2 M aniline in NMP (Table 3, $\sigma \leq 0$). In the absence of $AgClO_4$, on-resin oxidation of an *N*-terminal *N*-(4-methoxyphenyl)glycine (Table 3, **3o**) was observed to give ~10% of the glyoxyl-peptoid in the timespan of the reaction, increasing to 16% after 8 h. Conversion to the α-oxo aldehyde and subsequent peptoid decomposition was found to occur over time when *N*-aryl

DOI: 10.1021/acs.joc.5b01449
J. Org. Chem. 2015, 80, 10490–10497

Table 3. Conversions of 2 to the Desired *N*-Aryl Glycine-Containing Pentapeptoid in NMP for EDG-Substituted Anilines with $\sigma \leq 0$

	aniline	σ	% conversion to **3**
3l	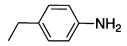	−0.151	97.6 ± 0.10[a]
3m	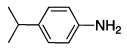	−0.151	95.0 ± 0.64[a]
3n	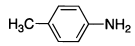	−0.170	94.6 ± 1.1[a]
3o	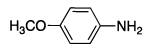	−0.268	98.3 ± 0.59[b]

[a]Reaction was stopped after 15 min. [b]Reaction was stopped after 10 min.

glycine-terminated peptoids were cleaved from the resin and kept in solution. Therefore, when electron-rich *N*-aryl glycine monomers are incorporated at the *N*-terminus, peptoids should be handled under air-free conditions and displacement reaction times should be kept to a minimum. Once such a peptoid is further elongated to embed the *N*-(EDG-aryl)glycines further in the peptoid sequence, stable products are obtained.

Mechanistic Investigation. In the two-step submonomer peptoid synthesis procedure, the substitution reaction between bromoacetylated peptoids and amines is presumed to proceed via an S_N2-type displacement mechanism, analogous to substitution reactions between α-halocarbonyls and nitrogen nucleophiles. The presence of a neighboring carbonyl group has been shown to significantly activate halides toward substitution reactions.[26] The high reactivity of these bielectrophilic compounds has been proposed to be due to stabilization of the transition state (TS) during nucleophile addition through delocalization toward the antibonding orbital of the neighboring carbonyl group $\pi^*_{C=O}$ (LUMO).[27] In previous work, in close analogy with the displacement reaction in submonomer peptoid synthesis (Figure 1b), nucleophilic substitution reactions of *N*-methyl α-bromoacetanilides with benzylamines were shown to involve complex mechanisms with either an enolate-like TS (Scheme 2a, TS I, Y = electron-withdrawing) or a five-membered hydrogen-bonded ring in the TS (Scheme 2b, TS II, Y = electron donating).[28]

To shed light on the mechanism of the displacement reaction in peptoid synthesis and elucidate the effect of silver salt addition, reaction rate constants were obtained. The conversions of bromoacetylated tetrapeptoid **2** to the desired *N*-aryl glycine product were plotted as a function of time in the presence and absence of silver perchlorate (see SI). The data were fitted to a pseudo-first-order reaction equation to obtain the rate constants, which were plotted against Hammett substituent constants ($\sigma-$)[29] (Figure 3a). Overall, addition of $AgClO_4$ during the displacement step with anilines accelerated the reactions by 8−76-fold (Figure 3b).

The observed negative slopes of the Hammett plots (Figure 3b) are indicative of a positive charge build-up on the incoming nucleophile in the transition state.[30] In the silver-mediated reaction, the less pronounced slope (−0.66 vs −2.1) signifies that there is less positive charge build-up on the nucleophile in the TS, suggesting that the nucleophile is better able to displace the leaving group, consistent with an improved leaving group capacity. This observation is consistent with electrophilic halide activation by silver perchlorate (Scheme 3). However, further studies would be necessary to discern between an enolate-like transition state or five-membered hydrogen-bonded ring in the transition state.

Addition of silver perchlorate with 4-aminobenzonitrile and other nonaromatic but weakly nucleophilic submonomers, such as 3-aminopentane and 1*H*,1*H*-perfluoropentylamine, did not improve reaction rates as compared to the unassisted displacement reaction in NMP. Therefore, it is likely that a cation−π interaction between the silver salt and the aniline nucleophile is necessary to efficiently promote the displacement reaction.

Synthesis of *N*-Aryl Glycine-Rich Peptoids. Using this methodology, we set out to prepare an extremely difficult peptoid sequence that contained five *N*-(4-trifluoromethylphenyl)glycine residues in a row, to explore the efficiency of this reaction in longer peptoid oligomers, as well as to establish the reaction times needed for complete aniline displacement following an electron-poor *N*-aryl glycine residue (Scheme 4). Using 3 equiv of $AgClO_4$ in THF for the displacement step with 1.2 M 4-(CF_3)aniline, nonapeptoid **12** was obtained as the major product (Figure 4a). Notably, while the first 4-(CF_3-phenyl)glycine incorporation required only a 1 h displacement time, subsequent incorporations needed 3−5 h to go to

Scheme 2. Postulated TS of Substitution Reactions between *N*-Methyl α-Bromoacetanilides and Benzylamines[27] Involving (a) a TS with Enolate Character and (b) a TS with a Five-Membered Hydrogen-Bonded Ring

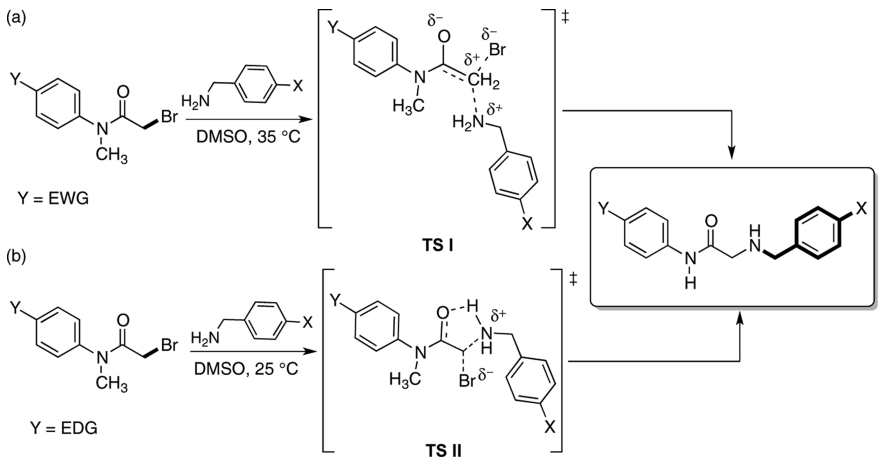

DOI: 10.1021/acs.joc.5b01449
J. Org. Chem. 2015, 80, 10490−10497

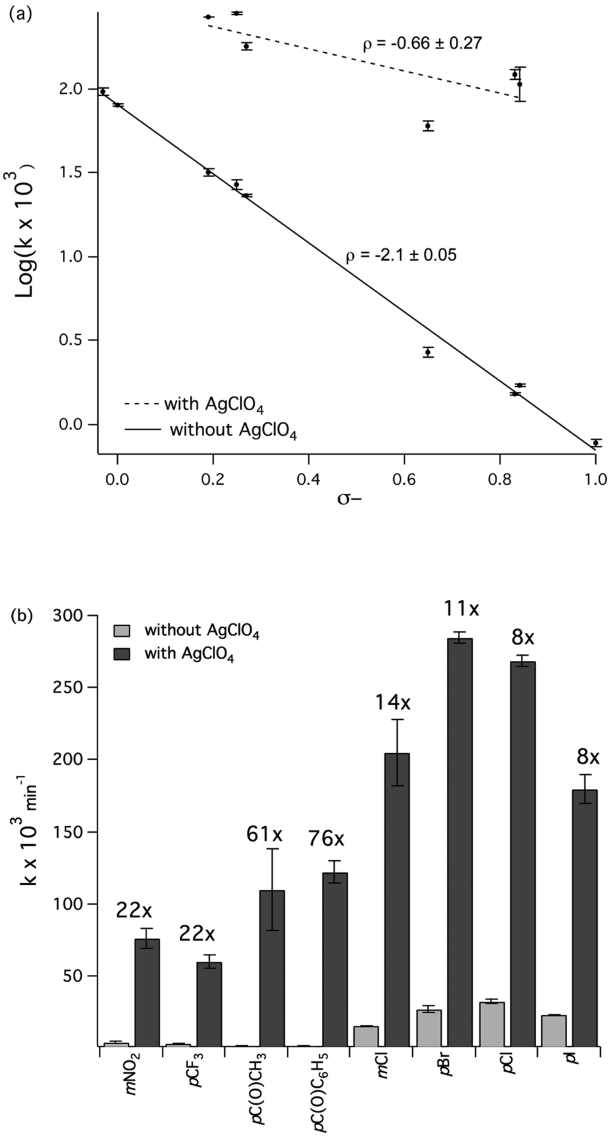

Figure 3. (a) Hammett plot with and without addition of $AgClO_4$. Of note, some of the displacement reactions proceeded too fast to accurately monitor, particularly in the presence of silver, and have been excluded from the Hammett plot. (b) Comparative reaction rate constants for substituted anilines using standard displacement conditions in NMP vs in the presence of silver perchlorate in THF. The numbers above the columns indicate the degree of rate acceleration using silver perchlorate relative to standard conditions in NMP.

Scheme 3. Postulated Role of Silver Perchlorate in Substitution Reactions between Bromoacetylated Peptoids and Amines

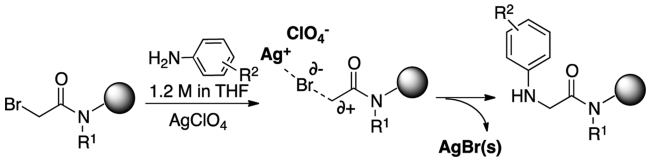

completion. Following a 4-(CF_3-phenyl)glycine residue, the bromoacetylation step was repeated twice (1 × 20 min, 1 × 60 min), requiring a total of 80 min. Purification using reversed-phase HPLC provided peptoid **12** in 13% yield. In comparison,

Scheme 4. Synthesis of Peptoid Oligomer 12

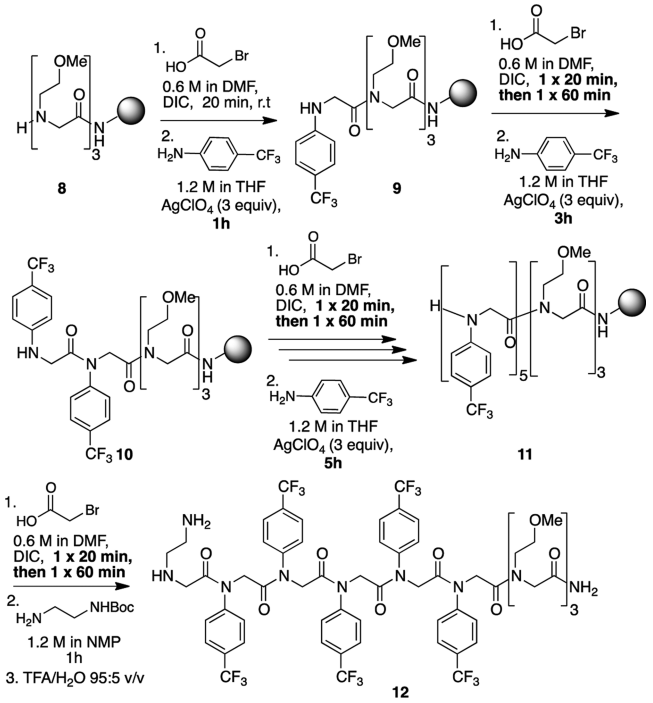

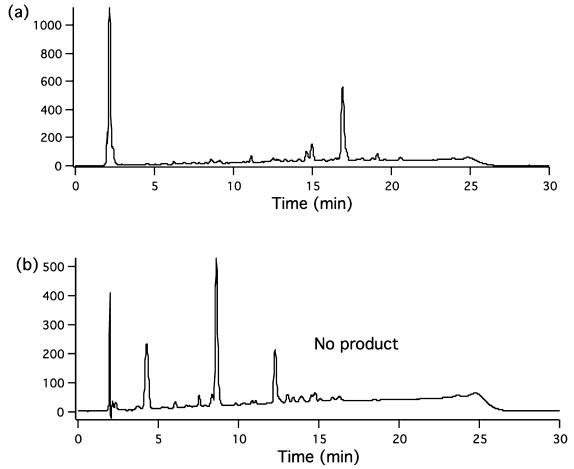

Figure 4. Comparative analytical HPLC traces of crude peptoid **12** synthesized using (a) 1.2 M 4-(CF_3)aniline in THF with 3 equiv of $AgClO_4$ and (b) 1.2 M 4-(CF_3)aniline in NMP, followed by cleavage from the resin.

the parallel synthesis of peptoid **12** using standard amine solutions in NMP and identical reaction times afforded no desired product (Figure 4b).

We next focused our attention on the synthesis of amphiphilic *N*-aryl glycine-rich peptoids **13a–d** (Figure 5), which have the potential to exhibit interesting self-assembling properties. For example, supramolecular assembly of amphiphilic peptoids into ordered, two-dimensional nanosheets has been shown to occur with a block-charged sequence that alternates with a 2-fold periodicity between aromatic and ionic monomers.[9] The introduction of *trans*-inducing *N*-aryl glycine residues is expected to favor an extended backbone configuration, as well as to restrict the side chain to $\chi^1 \approx 90°$.[5,10] This ability to limit conformational freedom in peptoid oligomers, coupled with our newfound capacity to engineer

DOI: 10.1021/acs.joc.5b01449
J. Org. Chem. 2015, 80, 10490−10497

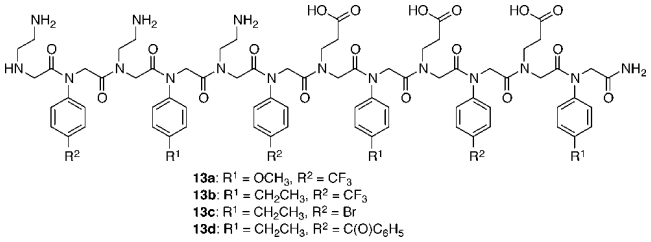

Figure 5. Structures of *N*-aryl glycine-rich peptoids **13a−d**.

better packing interactions between aromatic residues, should allow for stabilization of existing nanostructures, as well as the design and discovery of novel materials.

Peptoid oligomers **13a−d**, possessing six *N*-aryl glycine residues, were designed to alternate between electron-rich and -poor *N*-aryl glycines to enhance potential side chain−side chain aromatic interactions. In addition, peptoids **13c** and **13d** were synthesized to introduce photoreactive *N*-(4-bromophenyl)glycine and *N*-(benzophenone)glycine residues, respectively. Using our optimized conditions, peptoids **13a−d** were synthesized using $AgClO_4$ in THF for every other aniline displacement reaction (when R = EWG), in order to keep the displacement times to 1 h or less (see SI). In all cases, the desired peptoids were obtained as the major products, with crude purities ranging from 18% to 43% (Table 4). Purification

Table 4. Yields and Purities of *N*-Aryl Glycine-Containing Dodecapeptoids 13a−13d

Peptoid	Crude purity (%)	Yield (%)[a]	Purity (%)[b]
13a	43	27	96
13b	32	19	>99
13c	39	22	98
13d	18	9	91

[a]Based on resin loading. [b]Analytical HPLC analyses were performed on a Vydac column (4.6 mm × 150 mm, 5 μm, C18) at 60 °C with a flow rate of 1.0 mL/min using a 20−80% gradient of CH_3CN (0.1% TFA) in water (0.1% TFA) over 20 min. HPLC traces were monitored at 214 nm.

was achieved using reversed-phase HPLC to afford peptoids **13a−d** in >90% purities, and in overall isolated yields of 9−27%. This demonstrates the utility of halogen abstraction to enable the rapid introduction of multiple electron-poor *N*-aryl glycines in longer peptoid oligomers. Considering that hundreds of substituted anilines are commercially available, this method should significantly expand the toolbox of submonomers amenable to solid-phase peptoid synthesis. The self-assembling properties of peptoids **13a−d** will be reported in due time.

CONCLUSION

The ease by which peptoids are synthesized via the solid-phase submonomer procedure has enabled them to become a widespread class of peptidomimetics, with applications ranging from drug discovery to design of robust nanomaterials. Here, an improvement to the well-established peptoid synthesis procedure was reported, enabling up to 76-fold rate enhancements during the displacement step using weak aniline nucleophiles. This methodology should significantly increase the diversity of submonomers routinely used in peptoid oligomers, allowing traditionally difficult monomers to be incorporated with short displacement times (≤1 h). Given the ability of *N*-aryl glycines to induce local conformational order in peptoids, this method allows for the simultaneous introduction of a structure-inducing residue and chemically diverse functionality. The precise patterning of electron-rich and -poor *N*-aryl glycines should allow for the design and discovery of novel structured peptoids. Furthermore, oxidation of electron-rich *N*-aryl glycine residues to afford glyoxyl-terminated peptoids, which can be achieved upon prolonged exposure to silver perchlorate, offers the potential to generate reactive handles for chemical ligation, as well as libraries of heterocycle-terminated peptoids.

EXPERIMENTAL SECTION

General. Solid-phase chemistry was performed using polystyrene Rink Amide resin (0.57 mmol/g) in filtration tubes equipped with caps and stopcocks. Analytical HPLC analyses were performed on a 5 μm, 150 mm × 4.6 mm C18 Vydac column at 60 °C with a flow rate of 1.0 mL/min using a 20−80% gradient, where solvent A = water [0.1% trifluoroacetic acid (TFA)] and solvent B = MeCN (0.1% TFA). LCMS analyses were performed on a 5 μm, 50 mm × 2.1 mm C18 Vydac column with a flow rate of 0.35 mL/min using a 3−100% gradient. When applicable, peptoid oligomers were purified on a semipreparative column (5 μm, 250 mm × 21.2 mm, C18 Vydac columnTM) with a flow rate of 15 mL/min. HPLC traces were monitored at 214 nm.

Materials. Bromoacetic acid, *N*,*N*′-diisopropylcarbodiimide (DIC), trifluoroacetic acid, TIPS, and all amine reagents were purchased from commercial sources and used without further purification. Silver perchlorate was dried by azeotrope evaporation with benzene and placed in a desiccator under vacuum with P_2O_5 to give a white solid that was stored in a desiccator wrapped with foil. Solvents were purchased from commercial sources.

Silver Perchlorate Promoted Synthesis of Pentapeptoids 3a−3g. To 20 mg of resin-bound tetrapeptoid **1** in a 1 mL fritted cartridge were added 500 μL of DMF. Resin was allowed to swell for 20 min before draining. 500 μL of a 0.6 M solution of bromoacetic acid and 43 μL (24 equiv) of DIC were added and allowed to react for 20 min. The resin was washed with DMF (3 × 1 mL) and THF (2 × 1 mL) before adding 500 μL of a 1.5 M solution of aniline in THF, followed by 142 μL of a 0.25 M stock solution of $AgClO_4$ in THF (3 equiv), in this order. The reaction was allowed to proceed for 1 h, after which the reagents were drained and the resin was washed with DMF (3 × 1 mL) and DCM (1 × 1 mL). A small amount of resin was treated with a 95:5 TFA/H_2O v/v mixture for 10 min, and the TFA cleavage solution was collected by filtering the resin through a disposable, polypropylene fritted cartridge. The filtrate was evaporated to dryness by blowing a gentle stream of nitrogen and redissolved in 1:1 MeCN/H_2O prior to analysis by HPLC and LC/MS. **3a:** HPLC (20−80% MeCN, 20 min) retention time = 11.92 min; LCMS (ESI) calcd for $C_{36}H_{49}N_7O_9$ $[M + Na]^+$ 770.4, found *m*/*z* 770.5; **3b:** HPLC (20−80% MeCN, 20 min) retention time = 13.80 min; LCMS (ESI) calcd for $C_{39}H_{49}F_3N_6O_7$ $[M + Na]^+$ 793.4, found *m*/*z* 793.5; **3c:** HPLC (20−80% MeCN, 20 min) retention time = 10.24 min; LCMS (ESI) calcd for $C_{40}H_{52}N_6O_8$ $[M + H]^+$ 745.4, found *m*/*z* 745.3; **3d:** HPLC (20−80% MeCN, 20 min) retention time = 12.53 min; LCMS (ESI) calcd for $C_{45}H_{54}N_6O_8$ $[M + H]^+$ 807.4, found *m*/*z* 808.2; **3e:** HPLC (20−80% MeCN, 20 min) retention time = 14.37 min; LCMS (ESI) calcd for $C_{44}H_{54}N_8O_7$ $[M + H]^+$ 807.4, found *m*/*z* 807.7; **3f:** HPLC (20−80% MeCN, 20 min) retention time = 12.60 min; LCMS (ESI) calcd for $C_{38}H_{49}ClN_6O_7$ $[M + H]^+$ 737.3, found *m*/*z* 737.3; **3g:** HPLC (20−80% MeCN, 20 min) retention time = 12.61 min; LCMS (ESI) calcd for $C_{38}H_{49}BrN_6O_7$ $[M + Na]^+$ 803.3, found *m*/*z* 805.4.

Silver Perchlorate Promoted Synthesis of Pentapeptoids 3h−3k. Synthesis was performed as above, with displacement times of 15 min. **3h:** HPLC (20−80% MeCN, 20 min) retention time = 12.48 min; LCMS (ESI) calcd for $C_{38}H_{49}ClN_6O_7$ $[M + H]^+$ 737.3, found *m*/*z* 737.4; **3i:** HPLC (20−80% MeCN, 20 min) retention time =

DOI: 10.1021/acs.joc.5b01449
J. Org. Chem. 2015, 80, 10490−10497

13.33 min; LCMS (ESI) calcd for $C_{38}H_{49}IN_6O_7$ $[M + H]^+$ 829.3, found m/z 829.0; **3j:** HPLC (20−80% MeCN, 20 min) retention time = 10.35 min; LCMS (ESI) calcd for $C_{38}H_{49}FN_6O_7$ $[M + H]^+$ 721.4, found m/z 721.4; **3k:** HPLC (20−80% MeCN, 20 min) retention time = 10.17 min; LCMS (ESI) calcd for $C_{44}H_{54}N_6O_7$ $[M + H]^+$ 703.4, found m/z 703.8.

Synthesis of Pentapeptoids 3l−3o. To 20 mg of resin-bound tetrapeptoid **1** in a 1 mL solid-phase cartridge were added 500 μL of DMF. Resin was allowed to swell for 20 min before draining the DMF. 500 μL of a 0.6 M solution of bromoacetic acid and 43 μL (24 equiv) of DIC were added and allowed to react for 20 min. The resin was washed with DMF (3 × 1 mL) before adding 500 μL of a 1.2 M solution of aniline in NMP. The reaction was allowed to proceed for 10−15 min, after which the reagents were drained and the resin was washed with DMF (3 × 1 mL) and DCM (1 × 1 mL). A small amount of resin was treated with a 95:5 TFA/H_2O v/v mixture for 10 min, and the TFA cleavage solution was collected by filtering the resin through a disposable, polypropylene fritted cartridge. The filtrate was evaporated to dryness by blowing a gentle stream of nitrogen and redissolved in 1:1 MeCN/H_2O prior to analysis by HPLC and LC/MS. **3l:** HPLC (20−80% MeCN, 20 min) retention time = 11.25 min; LCMS (ESI) calcd for $C_{40}H_{54}N_6O_7$ $[M + H]^+$ 731.4, found m/z 731.9; **3m:** HPLC (20−80% MeCN, 20 min) retention time = 12.08 min; LCMS (ESI) calcd for $C_{41}H_{56}N_6O_7$ $[M + H]^+$ 745.4, found m/z 745.7; **3n:** HPLC (20−80% MeCN, 20 min) retention time = 10.29 min; LCMS (ESI) calcd for $C_{39}H_{52}N_6O_7$ $[M + H]^+$ 717.4, found m/z 717.8; **3o:** HPLC (20−80% MeCN, 20 min) retention time = 9.44 min; LCMS (ESI) calcd for $C_{39}H_{52}N_6O_8$ $[M + H]^+$ 733.4, found m/z 733.8.

Rate Constant Determination. To determine reaction kinetics, aliquots of resin were taken at different time intervals. Peptoids were cleaved from the resin as described above and analyzed by RP-HPLC. % Conversions were plotted as a function of time, and the data were fitted to a pseudo-first-order reaction equation: $f(x) = 100(1 - e^{-kt})$.[31]

Synthesis of Peptoid 12. Synthesis of tripeptoid **8** was accomplished using standard solid-phase submonomer peptoid synthesis procedures.[3] Incorporation of 4-(trifluoromethyl)aniline submonomers was accomplished using the representative silver-promoted displacement procedure described above, using a 1 h displacement time for the first incorporation, and 3−5 h displacement times for all subsequent incorporations. Washing of the silver bromide precipitate and bromoacetylation following a 4-(trifluoromethylphenyl)glycine residue was achieved by treating the resin with 500 μL of a 0.6 M solution of bromoacetic acid and 43 μL (24 equiv) of DIC for 20 min, draining the reagents, and repeating the bromoacetylation procedure for 60 min. Upon completion of the synthesis, the resin was washed with DMF (3 × 1 mL) and DCM (3 × 1 mL) and treated with a 95:5 TFA/H_2O v/v mixture for 2 h. The TFA cleavage solution was collected by filtering the resin through a disposable, polypropylene fritted cartridge, and the filtrate was evaporated to dryness using a Biotage V10 evaporator. The crude peptoid was redissolved in 40% MeCN in H_2O and purified by reversed-phase HPLC using a 40−90% gradient MeCN in H_2O over 60 min with a 15 mL/min flow rate, affording peptoid **12** as a white powder after lyophilization (13% yield). **12:** HPLC (20−80% MeCN, 20 min) retention time = 16.93 min; LCMS (ESI) calcd for $C_{64}H_{68}F_{15}N_{11}O_{12}$ $[M + H]^+$ 1469.3, found m/z 1469.5.

Synthesis of Peptoids 13a−d. Electron-rich aniline submonomers (4-ethylaniline, 4-methoxyaniline) were incorporated using standard 1.2 M solutions in NMP with a 3 h displacement time for the first incorporation and 1 h displacement times for subsequent incorporations. Bromoacetylation following an electron-rich *N*-aryl glycine monomer was performed for 2 × 20 min. Electron-poor aniline submonomers (4-trifluoromethylaniline, 4-bromoaniline, and 4-aminobenzophenone) were incorporated using the representative silver-promoted displacement procedure described above. Washing of the silver bromide precipitate and bromoacetylation following an electron-poor *N*-aryl glycine residue was achieved by treating the resin with 500 μL of a 0.6 M solution of bromoacetic acid and 43 μL (24 equiv) of DIC for 20 min, draining the reagents, and repeating the bromoacetylation procedure for 60 min. Cleavage from the resin and purification afforded peptoids **13a−d**: **13a** (27% yield): HPLC (20−80% MeCN, 20 min) retention time = 10.4 min; LCMS (ESI) calcd for $C_{81}H_{93}F_9N_{16}O_{21}[M + 2H]^+$ 899.8 found m/z 900.1; **13b** (19% yield): HPLC (20−80% MeCN, 20 min) retention time = 12.5 min; LCMS (ESI) calcd for $C_{84}H_{99}F_9N_{16}O_{18}$ $[M + 2H]^+$ 896.9, found m/z 897.3; **13c** (22% yield): HPLC (20−80% MeCN, 20 min) retention time = 11.4 min; LCMS (ESI) calcd for $C_{81}H_{99}Br_3N_{16}O_{18}$ $[M + 2H]^+$ 913.2, found m/z 913.8; **13d** (9% yield): HPLC (20−80% MeCN, 20 min) retention time = 12.1 min; LCMS (ESI) calcd for $C_{102}H_{114}N_{16}O_{21}$ $[M + 2H]^+$ 951.0, found m/z 951.6.

■ ASSOCIATED CONTENT

Supporting Information

The Supporting Information is available free of charge on the ACS Publications website at DOI: 10.1021/acs.joc.5b01449.

Representative protocol for the synthesis of peptoid **13b**; LCMS trace of peptoid **7**; % conversion vs time plots for pentapeptoids with and without $AgClO_4$ addition, fitted to a pseudo-first-order reaction equation; representative RP-HPLC traces for peptoid oligomers **3a−3o**; reversed-phase HPLC traces of crude and purified peptoid **13a−d** (PDF)

■ AUTHOR INFORMATION

Corresponding Author

*E-mail: rnzuckermann@lbl.gov.

Notes

The authors declare no competing financial interest.

■ ACKNOWLEDGMENTS

The authors thank J. W. Keillor, E. J. Robertson, and C. Tajon for helpful discussions. This work was supported by the Defense Threat Reduction Agency under Contract No. DTRA10027-15875, and the DARPA Fold F(x) program. The work was conducted at the Molecular Foundry with support by the Office of Science, Office of Basic Energy Sciences, U.S. Department of Energy, under Contract No. DE-AC02-05CH11231. C. P. is grateful for a postdoctoral fellowship from the Natural Sciences and Engineering Council of Canada (NSERC).

■ REFERENCES

(1) For a review, see: Sun, J.; Zuckermann, R. N. *ACS Nano* **2013**, *7*, 4715−4732.

(2) Miller, S. M.; Simon, R. J.; Ng, S.; Zuckermann, R. N.; Kerr, J. M.; Moos, W. H. *Drug Dev. Res.* **1995**, *35*, 20−32.

(3) Zuckermann, R. N.; Kerr, J. M.; Kent, S. B. H.; Moos, W. H. *J. Am. Chem. Soc.* **1992**, *114*, 10646−10647.

(4) Knight, A. S.; Zhou, E. Y.; Francis, M. B.; Zuckermann, R. N. *Adv. Mater.* **2015**, 1−27.

(5) Crapster, J. A.; Guzei, I. A.; Blackwell, H. E. *Angew. Chem., Int. Ed.* **2013**, *52*, 5079−5084.

(6) Huang, K.; Wu, C. W.; Sanborn, T. J.; Patch, J. A.; Kirshenbaum, K.; Zuckermann, R. N.; Barron, A. E.; Radhakrishnan, I. *J. Am. Chem. Soc.* **2006**, *128*, 1733−1738.

(7) For examples, see: (a) Wu, C. W.; Sanborn, T. J.; Huang, K.; Zuckermann, R. N.; Barron, A. E. *J. Am. Chem. Soc.* **2001**, *123*, 6778−6784. (b) Stringer, J. R.; Crapster, J. A.; Guzei, I. A.; Blackwell, H. E. *J. Am. Chem. Soc.* **2011**, *133*, 15559−15567.

(8) Murnen, H. K.; Rosales, A. M.; Jaworski, J. N.; Segalman, R. A.; Zuckermann, R. N. *J. Am. Chem. Soc.* **2010**, *132*, 16112−16119.

(9) (a) Nam, K. T.; Shelby, S. A.; Choi, P. H.; Marciel, A. B.; Chen, R.; Tan, L.; Chu, T. K.; Mesch, R. A.; Lee, B. C.; Connolly, M. D.; Kisielowski, C.; Zuckermann, R. N. *Nat. Mater.* **2010**, *9*, 454−460. (b) Kudirka, R.; Tran, H.; Sanii, B.; Nam, K. T.; Choi, P. H.;

DOI: 10.1021/acs.joc.5b01449
J. Org. Chem. 2015, 80, 10490−10497

Venkateswaran, N.; Chen, R.; Whitelam, S.; Zuckermann, R. N. *Biopolymers* **2011**, *96*, 586−595. (c) Sanii, B.; Kudirka, R.; Cho, A.; Venkateswaran, N.; Olivier, G. K.; Olson, A. M.; Tran, H.; Harada, R. M.; Tan, L.; Zuckermann, R. N. *J. Am. Chem. Soc.* **2011**, *133*, 20808−20815. (d) Olivier, G. K.; Cho, A.; Sanii, B.; Connolly, M. D.; Tran, H.; Zuckermann, R. N. *ACS Nano* **2013**, *7*, 9276−9286.

(10) (a) Paul, B.; Butterfoss, G. L.; Boswell, M. G.; Huang, M. L.; Bonneau, R.; Wolf, C.; Kirshenbaum, K. *Org. Lett.* **2012**, *14*, 926−929. (b) Shah, N. H.; Butterfoss, G. L.; Nguyen, K.; Yoo, B.; Bonneau, R.; Rabenstein, D. L.; Kirshenbaum, K. *J. Am. Chem. Soc.* **2008**, *130*, 16622−16632. (c) Stringer, J. R.; Crapster, J. A.; Guzei, I. A.; Blackwell, H. E. *J. Org. Chem.* **2010**, *75*, 6068−6078. (d) Paul, B.; Butterfoss, G. L.; Boswell, M. G.; Renfrew, P. D.; Yeung, F. G.; Shah, N. H.; Wolf, C.; Bonneau, R.; Kirshenbaum, K. *J. Am. Chem. Soc.* **2011**, *133*, 10910−10919.

(11) Salonen, L. M.; Ellermann, M.; Diederich, F. *Angew. Chem., Int. Ed.* **2011**, *50*, 4808−4842.

(12) (a) Claessens, C. G.; Stoddart, J. F. *J. Phys. Org. Chem.* **1997**, *10*, 254−272. (b) McGaughey, G. B.; Gagné, M.; Rappé, A. K. *J. Biol. Chem.* **1998**, *273*, 15458−15463.

(13) Roy, O.; Caumes, C.; Esvan, Y.; Didierjean, C.; Faure, S.; Taillefumier, C. *Org. Lett.* **2013**, *15*, 2246−2249.

(14) Jordan, P. A.; Bishwajit, P.; Butterfoss, G. L.; Renfrew, P. D.; Bonneau, R.; Kirshenbaum, K. *Biopolymers* **2011**, *96*, 617−626.

(15) Crapster, J. A.; Stringer, J. R.; Guzei, I. A.; Blackwell, H. E. *Biopolymers* **2011**, *96*, 604−616.

(16) Sarma, B. K.; Kodadek, T. *ACS Comb. Sci.* **2012**, *14*, 558−564.

(17) (a) Gorske, B. C.; Stringer, J. R.; Bastian, B. L.; Fowler, S. A.; Blackwell, H. E. *J. Am. Chem. Soc.* **2009**, *131*, 16555−16567. (b) Gorske, B. C.; Blackwell, H. E. *J. Am. Chem. Soc.* **2006**, *128*, 14378−14387. (c) Fowler, S. A.; Luechapanichkul, R.; Blackwell, H. E. *J. Org. Chem.* **2009**, *74*, 1440−1449. (d) Gorske, B. C.; Bastian, B. L.; Geske, G. D.; Blackwell, H. E. *J. Am. Chem. Soc.* **2007**, *129*, 8928−8929.

(18) Shah, N. H.; Kirshenbaum, K. *Org. Biomol. Chem.* **2008**, *6*, 2516−2521.

(19) Weibel, J. M.; Blanc, A.; Pale, P. *Chem. Rev.* **2008**, *108*, 3149−3173.

(20) (a) Pocker, Y.; Wong, W. H. *J. Am. Chem. Soc.* **1975**, *97*, 7097−7104. (b) Pocker, Y.; Wong, W. H. *J. Am. Chem. Soc.* **1975**, *97*, 7105−7109. (c) Kornblum, N.; Smiley, R. A.; Blackwood, R. K.; Iffland, D. C. *J. Am. Chem. Soc.* **1955**, *77*, 6269−6280. (d) Pocker, Y. *J. Chem. Soc.* **1960**, 1972−1977. (e) Pocker, Y. *J. Chem. Soc.* **1959**, 1179−1183. (f) Pocker, Y.; Kevill, D. N. *J. Am. Chem. Soc.* **1965**, *87*, 5060−5067. (g) Pocker, Y.; Kevill, D. N. *J. Am. Chem. Soc.* **1965**, *87*, 4760−4770. (h) Pocker, Y.; Kevill, D. N. *J. Am. Chem. Soc.* **1965**, *87*, 4771−4777. (i) Pocker, Y.; Kevill, D. N. *J. Am. Chem. Soc.* **1965**, *87*, 4778−4781. (j) Winstein, S.; Ingraham, L. L. *J. Am. Chem. Soc.* **1955**, *77*, 1738−1743. (k) Godina, T. A.; Lubell, W. D. *J. Org. Chem.* **2011**, *76*, 5846−5849.

(21) For a selected recent example, see: Lebrasseur, N.; Larrosa, I. *J. Am. Chem. Soc.* **2008**, *130*, 2926−2927.

(22) For selected examples, see: (a) Barbe, G.; St-Onge, M.; Charette, A. B. *Org. Lett.* **2008**, *10*, 5497−5499. (b) Jean-Gerard, L.; Pauvert, M.; Collet, S.; Guingant, A.; Evain, M. *Tetrahedron* **2007**, *63*, 11250−11259. (c) Krow, G. R.; Lin, G. L.; Yu, F.; Sonnet, P. E. *Org. Lett.* **2003**, *5*, 2739−2741. (d) Grant, T. N.; West, F. G. *J. Am. Chem. Soc.* **2006**, *128*, 9348−9349.

(23) Pasto, D. J.; Garves, K. *J. Org. Chem.* **1967**, *32*, 778−781.

(24) Santini, R.; Griffith, M. C.; Qi, M. *Tetrahedron Lett.* **1998**, *39*, 8951−8954.

(25) To assess the solubility of AgBr in the subsequent acylation step, reagent grade AgBr (8 mg, 0.043 mmol) was added to a solution of 0.6 M bromoacetic acid in DMF (1 mL). After 20 min of stirring, the yellow solid was found to completely dissolve. Our protocol generates <0.043 mmol of AgBr/mL of 0.6 M bromoacetic acid solution in DMF.

(26) (a) Conant, J. B.; Kirner, W. R.; Hussey, R. E. *J. Am. Chem. Soc.* **1925**, *47*, 488−501. (b) Bordwell, F. G.; Brannen, W. T. *J. Am. Chem. Soc.* **1964**, *86*, 4645−4650.

(27) (a) Lee, K. S.; Adhikary, K. K.; Lee, H. W.; Lee, B. S.; Lee, I. *Org. Biomol. Chem.* **2003**, *1*, 1989−1994. (b) Morkovnik, A. S.; Divaeva, L. N.; Anisimova, V. A. *Russ. Chem. Bull.* **2007**, *56*, 1194−1209. (c) Adhikary, K. K.; Kim, C. K.; Lee, B. S.; Lee, H. W. *Korean J. Chem. Eng.* **2008**, *29*, 191−196.

(28) Adhikary, K. K.; Lee, H. W. *Bull. Korean Chem. Soc.* **2011**, *32*, 857−862.

(29) Hansch, C.; Leo, A.; Taft, R. W. *Chem. Rev.* **1991**, *91*, 165−195.

(30) Isaacs, N. *Physical Organic Chemistry*; Wiley: New York, 1995.

(31) Yan, B.; Fell, J. B.; Kumaravel, G. *J. Org. Chem.* **1996**, *61*, 7467−7472.

DOI: 10.1021/acs.joc.5b01449
J. Org. Chem. 2015, 80, 10490−10497